Effect of nitrogen addition on the properties of C:F thin films deposited by RF sputtering

P. Gonon

Effect of nitrogen addition on the properties of C:F thin films deposited by RF sputtering

P. Gonon[a]

Laboratory for Electrostatics and Dielectric Materials (LEMD), French National Centre for Scientific Research (CNRS) and Joseph Fourier University (UJF), LEMD-CNRS, BP 166, 38042 Grenoble Cedex 9, France

Abstract. Fluorocarbon (C:F) and nitrogen-doped fluorocarbon (C:F:N) thin films are deposited by RF magnetron sputtering using a polytetrafluoroethylene (PTFE) target and Ar or Ar/N_2 sputtering gas. Properties of C:F:N films are compared to those of C:F films. They are studied using X-ray Photoelec-tron Spectroscopy (XPS), Infra-Red (IR) transmission spectroscopy, Thermo-Gravimetric Analysis (TGA), impedance spectroscopy, and current-voltage measurements. By adding nitrogen to the sputtering gas, XPS shows that nitrogen substitutes for fluorine leading to a decrease in the relative concentration of CF_x species, to an increase in C-C bonds, and to the appearance of specific CFN bonds. There is also a new IR band at 1350 cm^{-1} whose origin is uncertain (CN bonds or disordered sp^2 carbon). Thermal stability is not improved upon nitrogen addition (the C:F and C:F:N films both decompose above 200 °C). Dielectric properties (dielectric constant and loss) are only slightly affected by nitrogen doping. The DC transport properties are modified upon nitrogen addition (C:F:N films display a higher resistivity and a supra-linear behaviour at high fields indicative of field-enhanced tunnelling transport).

1 Introduction

The electronic packaging industry is continuously seeking dielectrics with improved performances to meet demands for faster circuits and higher integration density. Needs are expressed at the Printed Circuit Boards (PCB) level, as well as at the package level (e.g. Multi Chip Modules, or MCM), for dielectrics with a low dielectric constant and low loss in order to allow fast signal propagation speed, low signal attenuation, and reduced cross-talk between adjacent lines [1]. Due to its low dielectric constant (2) and very low loss factor ($\sim 10^{-4}$), poly-tetrafluoroethylene (PTFE, also named Teflon^{TM}) is a dielectric of choice for such applications. It is now a well accepted dielectric in the packaging industry where it is used, for instance, for the fabrication of high-frequency PCB [2]. PTFE is a crystalline polymer made of -(CF_2)- monomers. Its low permittivity results from the symmetry of the F-C-F monomer (absence of dipole at the molecular level) and from the strong electronegativity of fluorine (reduced ionic and electronic polarisations). PTFE melts at 327 °C, a temperature high enough to withstand temperature peaks encountered during package processing (such as the soldering step which usually takes place around 250 °C for lead-free packages).

Most of the substrates used in electronic packaging (PCB and MCM) are fabricated using lamination processes. Lamination is an additive process where thick dielectric sheets (with proper surface metallization) are hot-pressed together to form a multi-layer structure. Present PTFE-based PCB are fabricated in this way. As the thickness of individual laminates is in the 100 μm range it is difficult to achieve lateral feature sizes lower than this dimension (a typical via diameter is in the 100 μm range). As the demand for higher and higher packaging density is progressing, there is a strong need for alternative technologies allowing the use of thin films. The major advantage of using thin films (in the 10 μm range, and below) is the possibility to decrease lateral feature sizes, by at least an order of magnitude, and to increase the integration density of PCB [1]. For such technologies PTFE films could find useful applications (high-frequency boards where low dielectric constant and low loss dielectrics are required).

A major problem with PTFE is the difficulty in depositing this material as thin films. PTFE cannot be readily dissolved, and therefore cannot be deposited by spin coating. Nano-emulsions of PTFE particles can be used for such a purpose [3], however, this technique requires sintering temperatures above the melting point of PTFE. Various CVD and PVD techniques were used in an attempt to deposit PTFE [4]. In the present work we are interested in the Radio-Frequency (RF) sputtering technique.

[a] e-mail: patrice.gonon@grenoble.cnrs.fr

The sputtering technique is now a well established technique in the packaging industry (e.g. for metal deposition) and its use for the deposition of dielectrics would require minimum technological investment. The first attempts to deposit PTFE films by sputtering were made in the early 1970s [5–7]. Unfortunately the sputtering technique invariably leads to a highly cross-linked and amorphous matrix (C:F, or "fluorocarbon" films). Though sometimes termed "polymeric", these films are not polymers and they completely lose the crystalline structure of PTFE. Nevertheless, C:F films keep some of the most interesting properties of PTFE, such as a low dielectric constant [6], a low refractive index [7], a low coefficient of friction [5], and hydrophobicity [8], to name a few. The main problem associated with fluorocarbon thin films are their poor thermal stability [9–15]. Pronounced material decomposition, accompanied with the desorption of CF_x species, is usually observed above 200 °C [10,13–15]. This precludes any application of C:F films above 200 °C. Physico-chemical mechanisms at the origin of material decomposition are not yet clearly understood. Past studies [11,12] show that films decomposition depends on many parameters (cross-linking density, presence of impurities within the films) related to the deposition conditions (substrate temperature, deposition technique, gas precursors, etc.) [9–15]. There were some claims of films stable up to 350 °C (grown by the helicon-wave plasma-enhanced CVD) [16], and even up to 400 °C (grown by electron cyclotron resonance CVD) [17], but such reports remain exceptions. There were also some reports on the fact that nitrogen incorporation in C:F films, through nitrogen doping during growth [18,19] or by means of post-deposition plasma treatment [20], could greatly improve their thermal stability. This improvement was postulated to be due to the formation of stable C-N bonds and to a higher cross-linking density [18]. In those works [18–20] the films were deposited by plasma-enhanced CVD. Regarding films deposited by sputtering, only a few works reported on the influence of nitrogen addition in the sputtering gas [21–23]. No mention was made of an improvement of thermal stability.

In the present work we investigated the influence of nitrogen addition on the properties of C:F films deposited by PTFE sputtering. C:F:N films were obtained by adding N_2 to the sputtering gas (Ar). Chemical bonds in C:F and C:F:N films were studied by X-ray Photoelectron Spectroscopy (XPS) and Infra-Red (IR) transmission spectroscopy. Thermal stability was assessed by Thermo-Gravimetric Analysis (TGA). Electrical properties were studied using impedance spectroscopy and DC conductivity measurements.

2 Experimental

The films were grown by RF magnetron sputtering using a PTFE target. Sputtering gas was either pure argon (100% Ar, leading to C:F films) or a mixture of argon and nitrogen (50% Ar and 50% N_2, leading to C:F:N films). In both cases gas pressure was maintained at 10^{-2} mbar. The target was 10 cm in diameter and was powered at 200 W. Substrates were mounted on a water-cooled substrate holder and were placed five cm apart from the target.

Films used for XPS analysis were grown on stainless steel substrates. XPS was performed using the MgK radiation (1253.6 eV) in a Vacuum Generator chamber. Some films were peeled off from stainless steel substrates and the material was used for TGA measurements. TGA was performed at 5 °C/min under flowing argon (Perkin Elmer analyser). Additional films grown on highly resistive silicon were used for IR transmission analysis (BioRad instrument).

Films used for electrical analysis were grown on aluminium coated silicon substrates. After film deposition, circular gold contacts (3 mm in diameter) were evaporated on the top film surface to form Au/C:F/Al or Au/C:F:N/Al structures. Both C:F and C:F:N films were 6 μm thick. Impedance measurements were performed with a Novocontrol analyser working from 0.1 Hz to 100 kHz at an effective voltage of 3 V (electric field of 5 kV/cm). DC currents were recorded with a Keithley 6517 electrometer with voltage biases ranging from 1 to 100 V (1.7 to 170 kV/cm). Unless specified, positive bias was applied on the aluminium electrode and the current was collected at the gold electrode. Electrical measurements were recorded with the samples maintained in a shielded cell whose temperature can be varied. Before each electrical measurement the sample cell is evacuated (primary vacuum) and filled with dry argon.

3 Results and discussion

3.1 Composition and chemical bonds

Films composition was determined by XPS. For C:F films (sputtered in 100% Ar) we measure 59% fluorine, 40% carbon and a little oxygen (1%). For C:F:N films (sputtered under 50% Ar + 50% N_2) we get 50% fluorine, 40% carbon, 2% oxygen, and 8% nitrogen. It clearly appears that nitrogen substitute for fluorine in the films, whereas the carbon concentration remains constant. The same observation was made by Endo and Tatsumi [18] for C:F:N films elaborated by plasma-enhanced CVD.

The nitrogen concentration (only 8%) remains quite low in view of the high concentration of N_2 in the gas phase (50%). This corroborates the results of Yokomichi [22] which was not able to incorporate more than 15% nitrogen (sputtering technique). Similar results where obtained by Endo and Tatsumi [18] who observed a saturation of the nitrogen concentration at about 13% (films elaborated by plasma-enhanced CVD). Differences in the value of maximum nitrogen concentrations (8%, 15% and 13%) are probably linked to the different deposition conditions. However, in any cases it seems difficult to incorporate more than about 10% nitrogen in C:F films (as a rough indicative value). This could arise from the nitrogen precursor (N_2) which possesses a strong nitrogen bond (low dissociation rate resulting in a few nitrogen radicals

Table 1. Deconvolution of the XPS C 1s core level spectrum for C:F and C:F:N films.

Energy (eV)	285.1	287.5	289.6	291.8	293.9	286.0	288.5	290.6	292.9
Attribution	C-C	C-CF_x	C-F	C-F_2	C-F_3	C-N	O=C-N	F-C-NF_2	F_2-C-NF_2
% in C:F	2.0	21.6	23.4	35.2	17.7	-	-	-	-
% in C:F:N	8.2	15.4	22.0	31.5	15.1	1.4	0.9	2.4	3.1

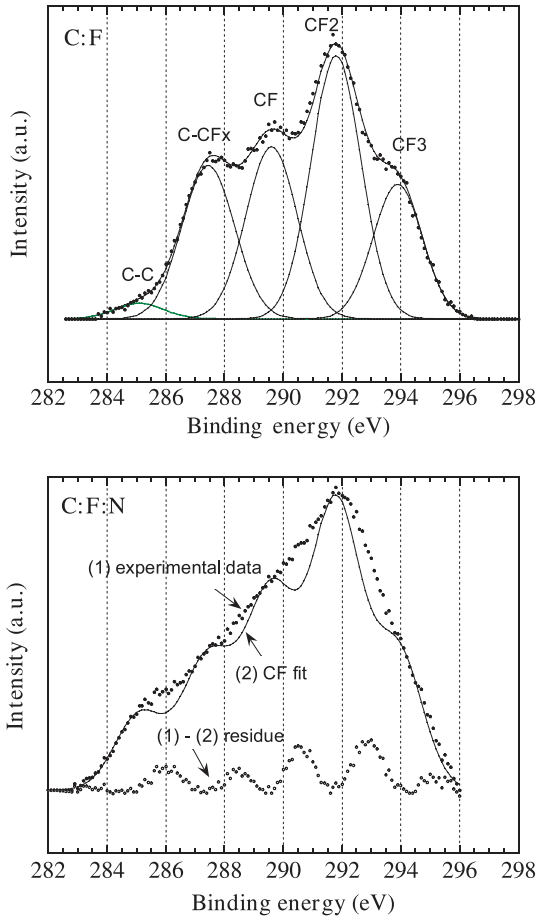

Fig. 1. XPS C1s core level spectra for C:F and C:F:N films. Dots are experimental points, lines are Gaussian fits. In the bottom figure (C:F:N) the experimental points (curve 1) are fitted using the same CF bands (curve 2) as for the top figure (C:F), and the residue is shown as the difference between curves 1 and 2.

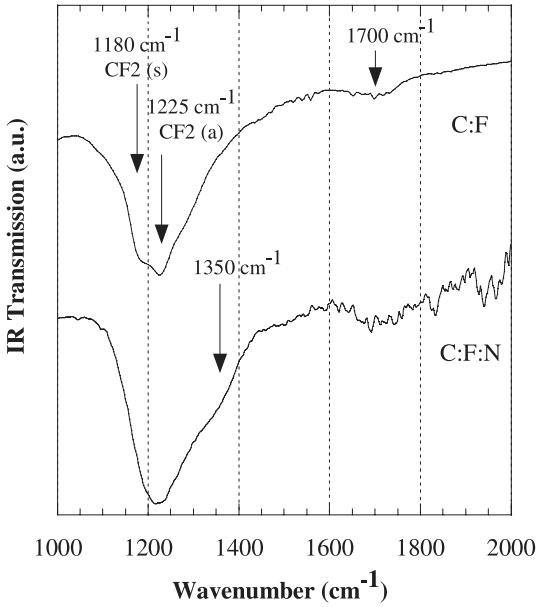

Fig. 2. FTIR transmission spectra of C:F and C:F:N films deposited on silicon.

in the gas phase). Alternatively, it could be due to the high electronegavity of fluorine which favours carbon-fluorine bonds over carbon-nitrogen bonds.

Figure 1 shows the XPS C1s core level spectra of C:F and C:F:N films. In C:F films we find the carbon-fluorine bonds usually found in such material, i.e. C-C, C-CF, C-F, C-F_2 and C-F_3 species [4]. Table 1 gives the peak position and percentage of these bonds. When adding nitrogen the C1s spectrum is strongly modified (Fig. 1), and we get a featureless band extending from 283 to 296 eV. The featureless nature of the C:F:N spectrum renders any unambiguous deconvolution difficult. Nevertheless, in an attempt to extract some information from this spectrum, we decided to proceed in the following manner. Firstly, we used the same carbon-fluorine components as the ones used for the deconvolution of C:F spectra. Their peak positions were fixed at the same energy, and their intensities were adjusted so that their sum fits the C:F:N experimental curve. In that way we obtain the contribution from the carbon-fluorine bonds alone (curve labelled "CF fit" in Fig. 1, C:F:N case). Secondly, carbon-fluorine components were subtracted from the C:F:N experimental curve, leaving a residue which is intended to represent the new bonds introduced by nitrogen doping (curve labelled "residue" in Fig. 1, C:F:N case). This procedure leaves new peaks at 286 eV, 288.5 eV, 290.6 eV, and 292.9 eV (see Tab. 1). According to the literature, the peak at 286 eV could be ascribed to CN bonds [24,25]. When comparing to the spectra of polyimide [24], the peak at 288.5 is possibly related to O=C-N groups. In C:F:N films Zhang and co-workers [23] also observed two peaks at 291 eV and 293 eV attributed to F-C-NF_2 and F_2-C-NF_2 species, respectively. Therefore, the peaks we observe at 290.6 eV and 292.9 eV could be ascribed to the same species.

IR transmission spectra are shown in Figure 2. In C:F films we observe bands at 1180, 1225 and 1700 cm^{-1}. The bands at 1180 cm^{-1} and 1225 cm^{-1} are ascribed to the symmetric and asymmetric vibrations of CF_2 groups [4]. The absorption at 1700 cm^{-1} has not a clear origin, it may be related to C=O or C=C bonds [4].

When adding nitrogen a shoulder appears at 1350 cm^{-1} (see Fig. 2). Such a band was already

reported in C:F:N material [22,23,26]. By analogy with the "D band" observed by Raman spectroscopy at about 1350 cm^{-1} in different forms of carbon [27], Yokomichi [22] attributed the IR band at 1350 cm^{-1} to disordered sp^2 carbon. The same interpretation was given in C:N materials where a similar absorption is observed around 1360 cm^{-1} [28,29]. Usually the Raman D band (ascribed by some authors to small-size graphitic domains [27]) is not observed to be IR active in carboneous materials. In C:N films it was argued that the D band becomes IR active by symmetry-breaking of the graphitic domains due to the incorporation of nitrogen [28,29]. A different origin for the 1350 cm^{-1} band was postulated by Zhang and co-workers who ascribed this band to CN bonds [23]. This would agree with the appearance of CN containing species detected by XPS (Tab. 1). If this interpretation is correct, then the C-N band in C:F:N would be quite far from the C-N band found in C:N materials (which was quoted at 1300 cm^{-1}) [29]. Such a shift should necessarily be related to the fluorine environment.

3.2 Thermal stability

To explain the observed enhancement of thermal stability for their C:F:N films, Endo and Tatsumi [18] invoked a reduction of C-F_x bonds (supposed to easily decompose upon annealing), a higher cross-linking density (more C-C bonds) and the presence of C-N bonds (supposed to be more stable than C-F bonds). In our films the addition of nitrogen indeed enhances the percentage of C-C bonds, lowers the percentage of CF_x groups (see Tab. 1), and possibly leads to C-N bonds (IR band at 1350 cm^{-1}). Therefore, according to previous arguments [18], we should expect the C:F:N films to be more thermally stable than the C:F films. The results of TGA analysis is depicted in Figure 3. We see that there is almost no improvement of thermal stability upon nitrogen incorporation. Decomposition of C:F:N and C:F films begins at the same temperature (around 200 °C). This observation is in a sharp contrast to the results of Endo and Tatsumi [18] who found that C:F:N films (13% nitrogen) were stable up to 300 °C.

The reason for such a discrepancy is unclear. As we have a film composition (40% C, 50% F, 8% N, 2% O) very close to the one of preceding authors (37% C, 50% F, 13% N) [18] we do not expect that the stoichiometry plays a significant role. It is more probable that the difference lies in the films structures, with the consequence that the mechanisms of thermal degradation are not the same in our films and in the films of Endo and Tatsumi [18]. For instance, as we have traces of oxygen in our films (2%), we cannot exclude that oxygen plays a significant role in our films. Oxygen was indeed suspected by several authors to reduce thermal stability through the decomposition of unstable oxygen containing moieties [11,13]. In that case nitrogen addition would be of no help in improving the thermal stability (because it would not impede the existence of unstable oxygen groups). It is also worth noting that Endo and Tatsumi [18] used a gas mixture containing hydrogen ($CF_4/N_2/CH_4$). Therefore, the observed difference

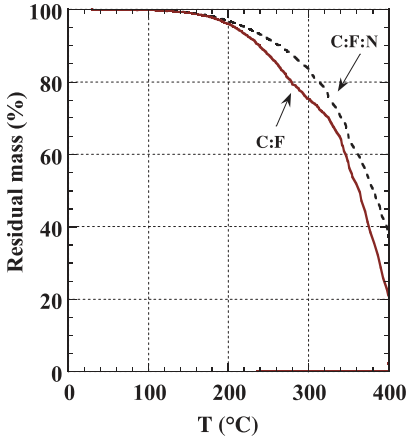

Fig. 3. TGA curves for C:F and C:F:N films (5 °C/min under Ar).

in thermal behaviour could also arise from the presence of hydrogen in their films. Thermal decomposition through HF elimination between neighbouring C-H and C-F bonds has been proposed to occur in hydrogen-containing fluorocarbons [11]. One can imagine that nitrogen, for instance by replacing some C-F groups by C-N(-H_x) species, could suppress such reactions (elimination of C-F groups participating in HF production). As we do not have hydrogen in the process, in our case the addition of nitrogen has no effect. These are speculative examples to illustrate what could be the differences between films chemistry and their possible implication on thermal behaviour. The contradictory results reported here demonstrate that the role of nitrogen in stabilising the films is not straightforward, and that adding nitrogen is not a guarantee of better thermal stability.

3.3 Dielectric properties

The real part of the permittivity (dielectric constant ε') and its imaginary part (loss factor ε'') are plotted in Figures 4 and 5.

For C:F films, at 100 kHz we measure $\varepsilon' \approx 2.5$ and $\varepsilon'' \approx 0.8 \times 10^{-2}$ (or a dissipation factor $\tan\delta = \varepsilon''/\varepsilon' = 3 \times 10^{-3}$). The low value of the dielectric constant results from the large amount of fluorine incorporated in the films (F/C=1.47 for C:F). The dielectric constant decreases with T (Fig. 4), while the loss increases with T with a pronounced rise at low frequencies (Fig. 5). We already reported a detailed investigation of the dielectric properties of C:F films [30]. Briefly, we concluded that in the 0.1−100 kHz range there are at least two relaxation processes. The first one (γ process) has a relaxation frequency above 100 kHz and therefore dominates the dielectric constant in the 0.1 Hz–100 kHz range. It is probably related to carbon-fluorine groups (orientational polarisation term). A second one (β process) has its relaxation frequency below 0.1 Hz. It is a much slower relaxation mechanism and it is responsible for the loss increase observed at low frequencies [30].

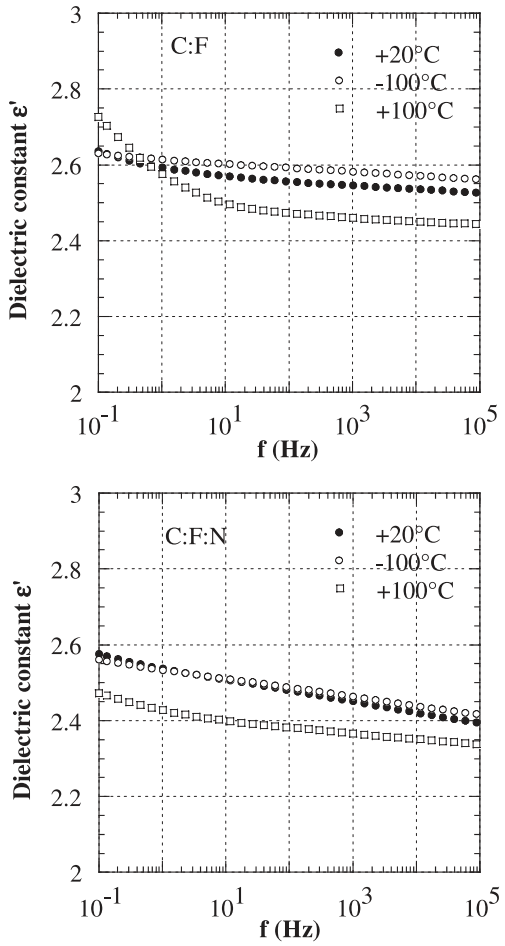

Fig. 4. Dielectric constant of C:F and C:F:N films as a function of frequency, for several temperatures.

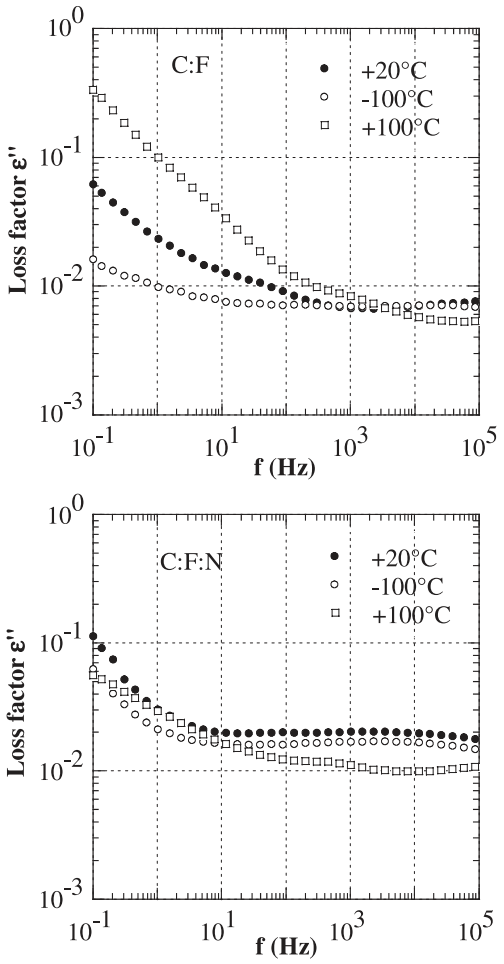

Fig. 5. Dielectric loss factor of C:F and C:F:N films as a function of frequency, for three temperatures.

When adding nitrogen (C:F:N in Figs. 4 and 5) at 100 kHz we have $\varepsilon' \approx 2.4$ and $\varepsilon'' \approx 2 \times 10^{-2}$ ($\tan\delta = 8 \times 10^{-3}$). Therefore we observe a very slight decrease in ε' upon nitrogen doping. The influence of F removal (through N addition) on the dielectric constant results from a balance of opposite effects, as explained below. Disappearance of fluorine increases the electronic polarisation term through the replacement of C-F bonds by more polarisable bonds such as C-N or C-C bonds. On the other hand, non-symmetric fluorine groups (C-F and $C\text{-}F_3$) possess a strong electric dipole and lead to a strong orientational polarisation term. Therefore, when C-F and $C\text{-}F_3$ groups disappear (F removal), the dielectric constant is decreased. In our films the last effect is probably the dominant one. This is consistent with the reduction of carbon-fluorine bonds (as observed in the present study by XPS) and the attribution of the γ process to these groups [30]. Other authors [18,23] observed the opposite trend, i.e. a slight increase in ε' after nitrogen doping. Again, the different behaviours are probably related to different films structures.

The increase in the loss at 100 kHz resulting from nitrogen addition agrees with the findings of Biderman [21] who observed the same trend. At 100 kHz the loss quoted here represents the background loss. It is dominated by secondary defects, which would mean that upon nitrogen addition the background concentration of electrical defects increases. This is consistent with the modification of the DC transport properties (see Sect. 3.4).

The temperature dependence of both the dielectric constant and the loss is less marked for C:F:N than for C:F films (Figs. 4 and 5). When compared to C:F, the low frequency relaxation term (β process) found in C:F:N appears to have a much weaker temperature dependence. This is clearly observed in Figure 5 (C:F:N case) where almost no change is observed in the low frequency part of the spectrum when the temperature is varied. This has to be related to a decrease in the activation energy of the very low frequency relaxation mechanisms. It is possible that the increase in cross-linking density (C-C bonds) is responsible for this effect (hindrance of dipolar chain movements due to an increase in network stiffness).

3.4 DC transport properties

Current-voltage characteristics recorded for C:F and C:F:N films are depicted in Figure 6. The C:F films show

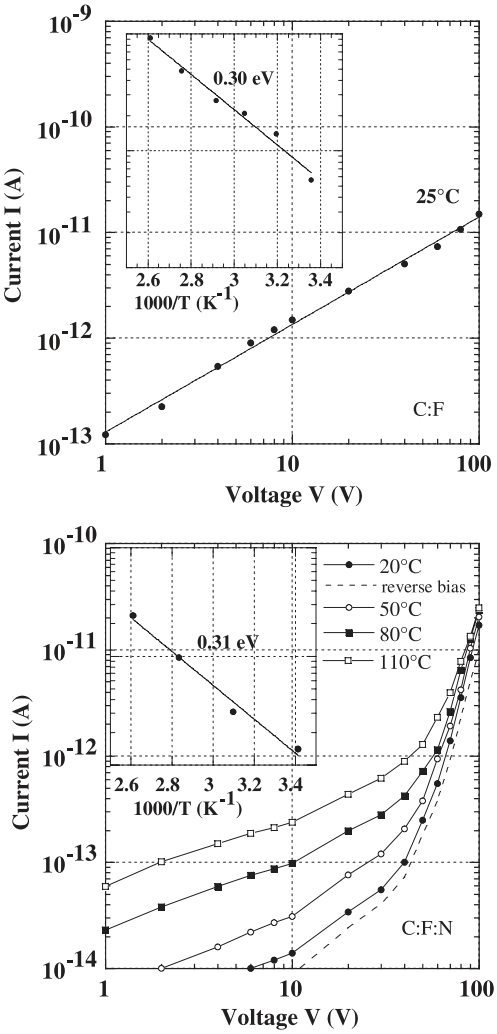

Fig. 6. Current-voltage characteristics for Au/C:F/Al (room temperature) and for Au/C:F:N/Al structures (different temperatures). Insets show the temperature dependence of the conductivity at 10 V. Positive bias is applied on the Al electrode, except for the dashed curve (C:F:N) where positive bias is applied on the Au electrode (reverse bias). Films thickness is 6 μm, contact diameter is 3 mm.

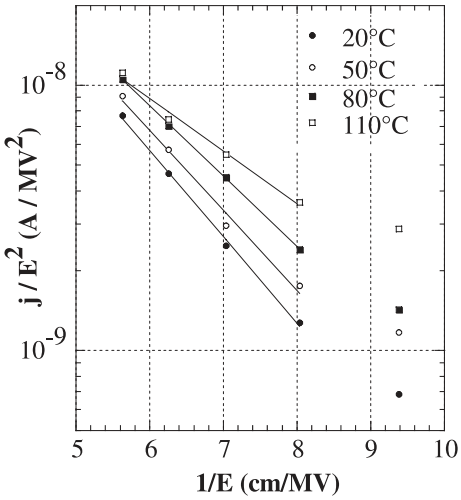

Fig. 7. Fowler-Nordheim plot of current-voltage characteristics obtained for C:F:N films (j is the current density and E is the electric field).

a linear (Ohmic) behaviour in the whole voltage range (100 V corresponds to a field of 170 kV/cm), at all temperatures. The resistivity of C:F films is around 10^{15} Ω.cm. Variation of resistivity with temperature (25−110 °C) is shown in the inset of Figure 6. We measure an activation energy of 0.30 eV.

In case of C:F:N films the current-voltage (I-V) characteristics are strongly non-linear (Fig. 6). Up to 30 V (50 kV/cm) we have an almost Ohmic behaviour. In this range the conductivity increases with temperature with an activation energy of 0.31 eV (see inset in Fig. 6 for C:F:N films). Above 30 V the current rises in a supralinear fashion. For the higher voltages (fields higher than 100 kV/cm) the I-V characteristics recorded at different temperatures tend to merge, i.e. the current is almost independent of temperature. Transport could be governed by the electrode/film interface, or it could be a bulk mechanism. As we have two different electrodes (Au on the top film surface, and Al on the back film side), in case of a transport controlled by the interface we could have expected to measure different I-V characteristics according to the bias polarity. This is not observed (I-V are almost symmetrical with respect to bias polarity, see Fig. 6). This seems to indicate that the transport in C:F:N films is controlled by the bulk.

The preceding behaviour (very large increase in current at high fields, almost independent of the temperature) is typical of field-enhanced tunnelling transport. Such a behaviour was reported several times in amorphous carbon films [31], as well as in semi-insulating amorphous semiconductors such as a-Si [32]. Several models were proposed (a brief review is given in [31]), most of them invoked field emission from traps within the bulk. A simple field emission process, which includes tunnelling, is the Fowler-Nordheim mechanism. For such a mechanism we have $I \sim AV^2 \exp(-B/V)$, where coefficients A and B depend on the barrier height ϕ through which carriers tunnel ($A \sim 1/\phi$ and $B \sim \phi^{3/2}$) [33]. Figure 7 shows the I-V characteristics replotted in a Fowler-Nordheim plot ($\mathrm{Ln}\, I/V^2$ as a function of $1/V$). A straight line is obtained for fields higher than 125 kV/cm ($1/E < 8$ cm/MV in Fig. 7), compatible with a Fowler-Nordheim type transport at high fields. Similar kind of analysis was conducted in a-Si [32] and in amorphous carbon [34]. Of course, the fact that some part of the data could be fitted to a Fowler-Nordheim law does not mean that this is the only mechanism that is able to explain the experiment (as pointed out by O'Dwyer [33], "it is notorious that different explanations can be advanced for high-field conduction properties, and that the type of explanation depends in large measure on the plots chosen to exhibit the experimental data"). Our analysis simply shows that Fowler-Nordheim type emission is a possible explanation.

In the Ohmic regime the conductivity of C:F:N is lower, by two decades, than the conductivity of C:F (see Fig. 6). Since C:F and C:F:N films display the same activation energy, it is likely that conduction is controlled by the same states which are located at 0.3 eV from the bands. A lower conductivity in C:F:N could result from a compensation of the these states by defects introduced during nitrogen doping (such a creation of defects is consistent with the increase in background loss observed in Fig. 5). During compensation the carriers originally located at the 0.3 eV levels are trapped at deeper levels from which they could be re-emitted by field-enhanced tunnelling into localised states (band tail) or into extended states (conduction band). Such mechanism was already proposed in another amorphous materials (a-Si and a-C) [31,34], and it could explain the occurrence of Fowler-Nordheim transport at high fields in C:F:N.

4 Summary and conclusions

The aim of this study was to investigate the effect of nitrogen addition on the properties of fluorocarbon films deposited by RF magnetron sputtering. When adding nitrogen to the gas phase nitrogen substitutes for fluorine, while the carbon content is maintained. New XPS bands are detected upon nitrogen doping, possibly related to C-N, F-C-NF_2 and F_2-C-NF_2 species. The percentage of C-C bonds and CF_x groups is lowered. An IR band also appears at 1350 cm^{-1} whose origin may be related to CN bonds or to disordered sp^2 carbon bonds.

Nitrogen addition does not improve the thermal stability of fluorocarbon thin films (deposited by the sputtering technique). The C:F and C:F:N films both decompose above 200 °C.

The dielectric properties are slightly affected by nitrogen addition (slight decrease of the dielectric constant and weak increase of loss). DC transport is much more strongly modified. Low-field resistivity is increased by two orders of magnitude. Transport becomes highly non-linear at high fields (Fowler-Nordheim type).

The author wishes to thank his colleagues at the University of Grenoble, namely G. Berthomé at "Laboratoire de Thermodynamique et Physicochimie Métallurgiques" for performing XPS analysis, J. Marcus at "Laboratoire des Propriétés Électroniques des Solides" for his help in TGA measurements, and E. Bustarret at Laboratoire des Propriétés Électroniques des Solides for FTIR analysis.

References

1. R.R. Tummala, *Fundamentals of Microsystems Packaging* (McGraw-Hill, New-York, 2001)
2. C.A. Harper, *High Performance Printed Circuit Boards* (McGraw-Hill, New-York, 2000)
3. R. Schwödiauer, G.S. Neugschwandtner, S. Bauer-Gogonea, S. Bauer, T. Rosenmayer, Appl. Phys. Lett. **76**, 2612 (2000)
4. A review is given by J. Theil, J. Vac. Sci. Technol. B **17**, 2397 (1999)
5. R. Harrop, P.J. Harrop, Thin Solid Films **3**, 109 (1969)
6. M. White, Thin Solid Films **18**, 157 (1973)
7. H. Biderman, S.M. Ojha, L. Holland, Thin Solid Films **41**, 329 (1977)
8. S. Agraharam, D.W. Hess, P.A. Kohl, S.A. Bidstrup Allen, J. Electrochem. Soc. **148**, F102 (2001)
9. A. Grill, V. Patel, C. Jahnes, J. Electrochem. Soc. **145**, 1649 (1998)
10. I. Banerjee, M. Harker, L. Wong, P.A. Coon, K.K. Gleason, J. Electrochem. Soc. **146**, 2219 (1999)
11. B. Cruden, K. Chu, K. Gleason, H. Sawin, J. Electrochem. Soc. **146**, 4590 (1999)
12. B. Cruden, K. Chu, K. Gleason, H. Sawin, J. Electrochem. Soc. **146**, 4597 (1999)
13. S. Agraharam, D.W. Hess, P.A. Kohl, S.A. Bidstrup Allen, J. Electrochem. Soc. **147**, 2665 (2000)
14. S.-S. Han, B.-S. Bae, J. Electrochem. Soc. **148**, F67 (2001)
15. H. Yokomichi, A. Masuda, Vacuum **59**, 771 (2000)
16. K. Endo, T. Tatsumi, Y. Matsubara, T. Horiuchi, Jpn J. Appl. Phys. **37**, 1809 (1998)
17. Y. Xin, S.-H. Xu, Z.-Y. Ning, X.-H. Lu, M.-F. Jiang, S. Huang, W. Du, J. Chen, C. Ye, S.-H. Cheng, Chin. Phys. Lett. **20**, 423 (2003)
18. K. Endo, T. Tatsumi, Appl. Phys. Lett. **68**, 3656 (1996)
19. L. Valentini, E. Braca, J.M. Kenny, G. Fedosenko, J. Engemann, L. Lozzi, S. Santucci, Thin Solid Films **408**, 291 (2002)
20. J.-M. Shieh, K.-C. Tsai, B.-T. Dai, S.-C. Lee, C.-H. Ying, Y.-K. Fang, J. Electrochem. Soc. **149**, G384 (2002)
21. H. Biederman, Vacuum **31**, 285 (1981)
22. H. Yokomichi, Recent Res. Devel. Appl. Phys. **4**, 113 (2001)
23. Y. Zhang, G.H. Yang, E.T. Kang, K.G. Neoh, W. Huang, A.C.H. Huan, S.Y. Wu, Langmuir **18**, 6373 (2002)
24. K.P. Adhi, R.L. Owings, T.A. Railkar, W.D. Brown, A.P. Malshe, Appl. Surf. Sci. **225**, 324 (2004)
25. D. Marton, K.J. Boyd, A.H. Al-Bayati, S.S. Todorov, J.W. Rabalais, Phys. Rev. Lett. **73**, 118 (1994)
26. H. Biederman, M. Zeuner, J. Zalman, P. Bilkova, D. Slavinska, V. Stelmasuk, A. Boldyreva, Thin Solid Films **392**, 208 (2001)
27. T.J. Dines, D. Tither, A. Dehbi, A. Matthews, Carbon **29**, 225 (1991)
28. S. Kobayashi, S. Nozaki, H. Morisaki, S. Fukui, S. Masaki, Thin Solid Films **281-282**, 289 (1996)
29. X.A. Zhao, C.W. Ong, Y.C. Tsang, Y.W. Wong, P.W. Chan, C.L. Choy, Appl. Phys. Lett. **66**, 2652 (1995)
30. P. Gonon, A. Sylvestre, J. Appl. Phys. **92**, 4584 (2002)
31. C. Godet, S. Kumar, V. Chu, Philos. Mag. **83**, 3351 (2003)
32. C.E. Nebel, R.A. Street, N.M. Johnson, C.C. Tsai, Phys. Rev. B **46**, 6803 (1992)
33. J.J. O'Dwyer, *The theory of electrical conduction and breakdown in solid dielectrics* (Clarendon Press, Oxford, 1973)
34. N.A. Hastas, C.A. Dimitriadis, D.H. Tassis, Y. Panayiotatos, S. Logothetidis, D. Papadimitriou, Appl. Phys. Lett. **79**, 3269 (2001)